SEMARAK ILMU PUBLISHING

Journal of Advanced Research in Fluid Mechanics and Thermal Sciences

Journal homepage:
https://semarakilmu.com.my/journals/index.php/fluid_mechanics_thermal_sciences/index
ISSN: 2289-7879

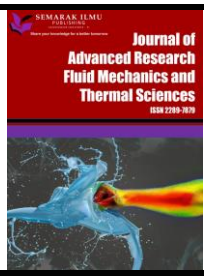

Experimental Investigation of Direct Solar Photovoltaics that Drives Absorption Refrigeration System

Jawad Khudhur[1], Abdulrazzak Akroot[1], Ahmed Al-Samari[2,*]

[1] Faculty of Engineering, Mechanical Engineering Department, Karabuk University, Turkey
[2] Faculty of Engineering, Mechanical Engineering Department, University of Diyala, Iraq

ARTICLE INFO

Article history:
Received 25 January 2023
Received in revised form 24 April 2023
Accepted 2 May 2023
Available online 20 May 2023

Keywords:
Diffusion absorption refrigeration; Ammonia-Water; renewable energy; technology PV system

ABSTRACT

Renewable energy used for refrigeration applications has become essential very recently due to the fossil fuel crisis and the global warming problem. Moreover, using photovoltaic PV to generate electricity than using inverters and energy storage represents a high-cost process. This study aims to investigate the opportunity of using PV output directly to operate a refrigeration system. The absorption refrigeration system uses heat as an energy source for the generator that drives the system. Moreover, the absorption refrigeration system doesn't have a compressor but a generator. As a result, the novel aspect of this study is the use of PV electricity's DC output to power the heater that provides the needed heat for the generator without the use of an inverter that provides AC electricity. The essential very difference here is that the compressor needs a consistent and steady electric supply. However, using DC electricity for heating is not very restricted if the voltage fluctuates a bit. A 580 W PV was used to power a refrigerator with a capacity of 70 liters. During several tests, the freezer of the fridge reached -26 C and the cabin temperature was around 10 C. This finding was similar to the performance of this fridge on a conventional heater.

1. Introduction

Solar energy is the most sustainable and cost-free way to manage the world's energy [1]. Moreover, the need for energy and its usage for cooling is growing as technology advances. Since the world population grows rapidly, thermal load loads increase increases, and living standards rise. In a world of increasing scarcity of primary energy. Furthermore, air-conditioning systems may be responsible for 60% to 80% of the energy consumed in commercial and public buildings [2]. Meanwhile, according to the BP statistical analysis of world energy (2017), fossil-based fuels account for the vast bulk of global energy use (85.5%) [3]. It is critical to seek alternatives to traditional energy sources [4]. Energy usage is directly related to economic growth and population. HVAC consumes 10-20% of the total energy usage in wealthy nations [5], and Solar energy is one of the most essential renewable energy sources. More specifically, because it is more commonly available via photovoltaic

* *Corresponding author.*
E-mail address: Ahmedshihab_eng@uodiyala.edu.iq

https://doi.org/10.37934/arfmts.106.1.116135

(PV) arrays and can be transformed into heat or mechanical energy with fair efficiency, it has been highlighted as a practical renewable energy source [4]. The recent global warming trend is escalating, with alarming alternative cooling methods being investigated to reduce the detrimental emissions of current systems [6]. Solar irradiation is a potential renewable energy source that can provide a large portion of human energy demand demands in a sustainable and viable manner [7, 8]. Solar-assisted cooling systems were discovered to save 40-50% of primary energy at a cost of 0.07€/kW [9]. Cooling systems can be classified based on the kind of input energy (for example, electrical or mechanical effort, solar, geothermal, or waste heat) or the processes connected with the thermodynamic cycle (e.g. vapour compression, adsorption, or absorption) [10]. A novel correlation is created to estimate the Coefficient of performance (COP) of single-effect VAR systems under different operating conditions. For the first time, the proposed correlation incorporates fluid characteristics such as absorbent and refrigerant boiling points [10]. Further classification can be formed based on cycle design, working fluid, or sorption medium. Absorption refrigeration is the most popular type of thermally driven system in the literature and on the market, with a wide range of cooling capabilities and cycle configurations. Finally, the pure refrigerant is condensed before being delivered as a liquid for evaporation, completing the cycle [7]. No moving components exist, and the refrigerating device operates according to Dalton's Law [11]. Absorption chillers and heat pumps are essential in energy efficiency and greenhouse gas reduction since they may be powered by waste heat or renewable energy. As a result, user confidence in these systems must be strengthened by increasing the volume and quality of operational data in real-world applications [12]. An absorption refrigerator employs a heat source (e.g., the sun, kerosene-fueled flame, waste heat from factories, or district heating systems) to power the cooling system. LiBr and NH3 are the two most commonly employed cycles in absorption (of ammonia and hydrogen). Water is now the absorbent, and NH3 is the refrigerant in an NH3 absorption system [13]. studied a double-stage absorption system using NH3/water and solar energy as the supply with nominal refrigeration power at 2 kW. The authors found a mean system COP at 0.21, while the maximum value at 0.25 [8]. The diffusion-absorption refrigeration cycle, often known as the DAR cycle, is an emerging field of research. The system's Coefficient of performance (COP) has been measured to fall somewhere between 0.12 to 0.26. Throughout the trials, the heat input to the DAR generator is maintained at a temperature ranging from 175-215 degrees Celsius. 30 percent is the mass concentration of ammonia in the working fluid combination [14]. The cycle runs at a single pressure level and employs three working fluids: a refrigerant, an absorbent, and an auxiliary gas utilized in the system to equalize pressure [15]. Ammonia, water, and hydrogen as inert gas are the most frequent working fluids. Helium was offered as a hydrogen alternative and experimented on an NH3-H2O DAR with helium as an auxiliary gas [16]. They also created a mathematical model to estimate the best operating parameters for optimal performance. They discovered that the mass transfer rates in the evaporator and absorber significantly impacted the system performance. The machine's COP was discovered to range between 0.09 and 0.15 [17]. Thai researchers have found that a configuration with partial subcooling had the highest COP. Different system configurations were investigated so that the performance coefficient was about 50% while keeping the cooling capacity constant [18]. Solar refrigeration may be produced in two ways: cycles with heat input and cycles with a photovoltaic. Heat-driven systems are typically used for air conditioning. Only absorption systems generate temperatures below zero degrees Fahrenheit for refrigeration applications. Some mathematical models predict a maximum COP of roughly 0.15 for such cycles, whereas practical observations indicate that COP coefficients can be improved up to 0.2 [19,20]. Nonetheless, the availability of free solar energy resources and vast unused land is quite promising when considering this strategy. In addition, permanent electricity in Iraq has existed for around thirty years, and no short-term remedy is anticipated. Consequently, this technology may aid

in reducing industrial and large buildings' reliance on grid power [21 22]. Malaysia's government has implemented policies to reduce electricity use by 20.7% of families using a refrigerator daily to encourage customers to use energy more wisely, as energy sustainability is essential for economic growth [23]. Developing nations must switch to renewable energy sources to secure energy security [24]. The relevance of developing solar-powered technology and boosting the usage of renewable energy sources is crucial for achieving these goals [25]. It may directly employ renewable energy resources or develop more appropriate energy sources [26].

This study aims to evaluate the chance of using solar energy for operating the refrigeration system for home use. The absorption refrigeration system using an energy source as heat would be invested to use photovoltaic (PV) to generate the direct electricity (DC) to operate the heater. The main advantage of using PV is to run the DC heater directly without using additional equipment to convert DC to AC electricity. Finally, this suggestion may help decrease the initial cost of the solar systems that generate the heat demanded to operate the refrigeration or air conditioning system. Figure 1 shows the absorption refrigeration cycle while Figure 2 shows the solar absorbtion refrigeration system.

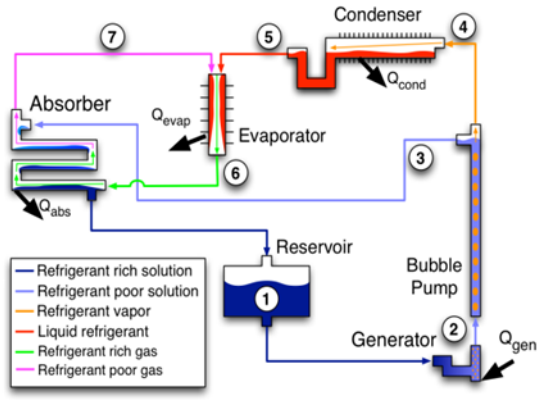

Fig. 1. A absorption refrigeration cycle

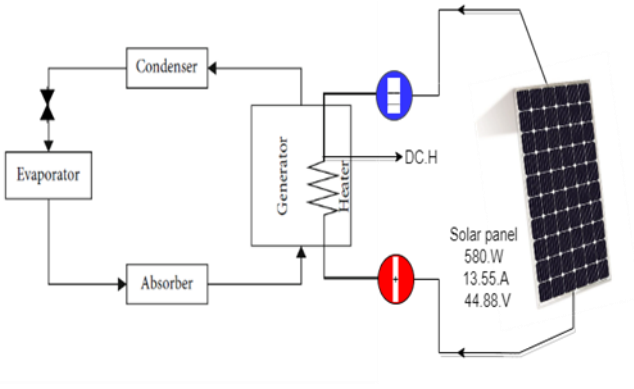

Fig. 2. Solar absorption refrigeration system

2. Description of Conventional Absorption Refrigeration System (ARS) And Solar - Assisted

View the basic ARS block diagram and components. The working fluid in the system chosen is H_2O-NH_3. Moreover, H_2O-NH_3 does not harm the environment in the same way that other commercial refrigerants do, and it does not crystallize below 0°C like Libr-H_2O. The heater is part of the system. The heater is a resistance load that can operate in both AC and DC without any design modifications, and the electrical power for the system will be provided by a 450 W solar PV panel. Solar energy is accessible all year round in a place like Iraq, so there is not much need for other additional energy.

2.1 Objective

The main objective of this project is to integrate solar photovoltaic energy into the Absorption Refrigeration System (ARS) directly without the use of a power converter that provides alternating current, which leads to a significant reduction in costs and the elimination of maintenance costs as well and to benefit from the lack of effect of voltage fluctuation on the heater that was designed for operating the system. Other objectives include calculating and comparing COP for solar ARS cycles and conventional ARS, as well as analyzing the temperature connection between the generator, evaporator, and other components.

3. Methodology

Figure 3 shows A diagram of (ARS) for ammonia and water, indicating the various components. The liquid solution with a high concentration of refrigerant is brought to the top of the bubble pump by heating it in the generator (1-2), generating vapor bubbles that climb higher. The liquid solution (3) travels downward in the outer shell of the bubble pump in the direction of the absorber, while the saturated vapor mixture (4) travels upward in the direction of the rectifier. The liquid and vapor phases are separated at the very top of the bubble pump. The rectifier's job is to remove any traces of water that may still be present in the vapor mixture via partial condensation. The liquid condensate emerges at the bottom of the rectifier (5). At the same time, the near-pure vapor refrigerant travels upwards to be condensed, causing heat to be released into the surrounding environment (6–7). The liquid refrigerant that is discharged from the condenser is precooled in the gas heat exchanger before it is allowed to proceed to the evaporator (7-9). (Specifically, hydrogen in this example). The phenomenon known as the refrigeration effect is caused by introducing the refrigerant into the hydrogen environment, which reduces the partial pressure of the substance and the subsequent occurrence of evaporation at low temperatures (9,10). After that, the vapor of the refrigerant is mixed with the inert gas, and this mixture is sent via the absorber. Within the absorber, the refrigerant vapor (10) is absorbed into the weak solution (8), which results in the release of heat and the production of a solution rich in refrigerant, which is then collected in the reservoir. This process is repeated (11). Since it is less dense than the refrigerant, the inert gas can rise to the top of the gas heat exchanger and then return to the evaporator.

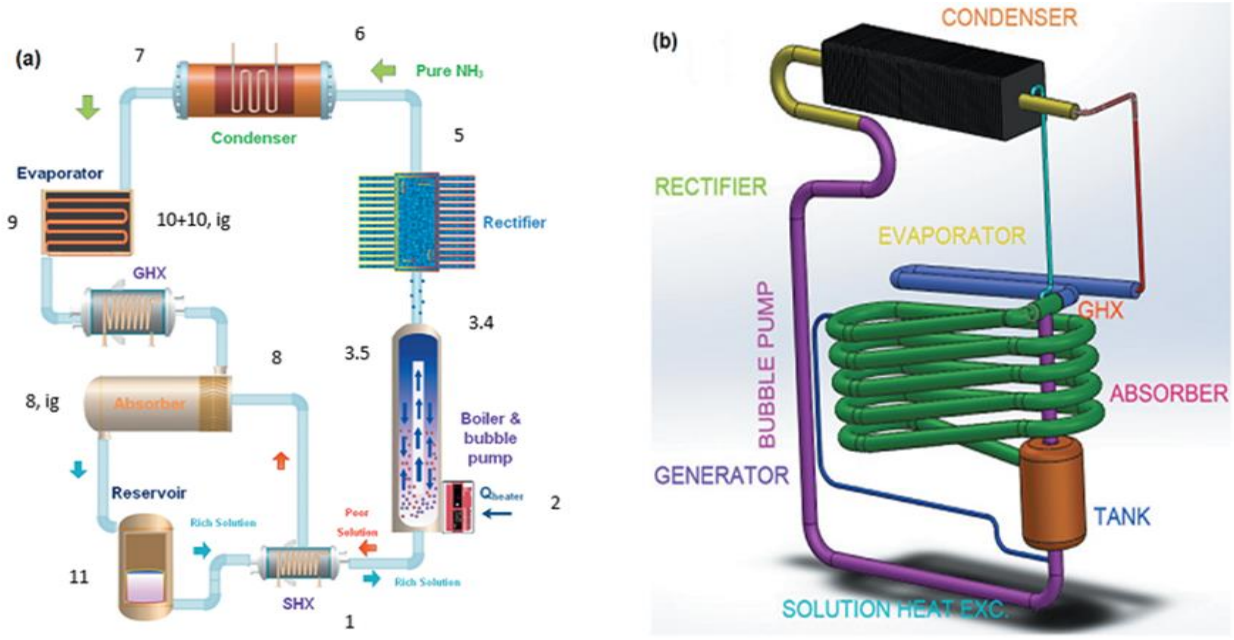

(a) (b)

Fig. 3. A schematic view of (a) the ARS system and (b) its refrigerator

3.1 Experimental Apparatus

Refrigeration based on photovoltaic (PV)-assisted aqueous ammonia absorption technology. As shown in Figure 1, during the experiments described in this paper, it was charged with a water-ammonia solution with a total mass concentration of thirty percent and hydrogen pressurized to 22 bar, according to the required by the default specifications provided by the manufacturer. It includes

a schematic representation of the SAR system. as shown in Figure 2 and a snapshot of the main parts of the system. As shown in Figure 4 and Figure 5, in addition to a schematic diagram of the components of the refrigerator, as shown in Figure 3. were used by the photovoltaic panel nominal power (+5w/-0w) Pump 580 W & Short circuit current Isc.13.55A with open circuit voltage.VOC,53.56V & Current at maximum power, Impp,12.92A & Voltage at maximum power, Vmpp, 44.88 V to drive the absorption cooling system with a capacity of 70 liters directly as shown in Figure 6. A DC heater designed and manufactured by us was used in the laboratory, with a length of 20 cm and a diameter of 12 mm. The outer cover of the heater is made of stainless steel, with a resistance wire with a diameter of 1.5 mm in the middle, where the resistance of the wire depends on 1 Ω per meter with a capacity of 48 volts and 450 watts. The total resistance of the heater is 5 Ω as shown in Figure 6, It is placed inside the generator next to the AC-powered heater. Thus, converting photovoltaic energy into heat energy directly drives S.SAR. This design was adapted to specifically target solar cooling applications in different climatic conditions (sunny, cloudy, dusty), in addition to that an inorganic thermal insulator of ceramic wool was used to isolate the generator from the inside to isolate it from the ambient temperature and not be affected by it, according to HP specifications 1260, with a density of (kg/m^3) with a thickness of 50 mm. Regather Ceramic Fiber is used between 750°C - 1430°C. Weave technology produces. Ceramic fibres consist of three basic elements; silica, alumina, and zirconium, a heat-insulating material for high temperatures. Some typical applications are industrial furnaces, boilers, stacks, places encountering high temperatures, kilns, reusable insulation for steam and gas turbines, lining for field steam generators, thermal reactor insulation, pressure and fire protection in cryogenic vessels. , which reflects positively on the system's response speed to work in less than 30 minutes, as shown in Figure 7, and electrical connections with a thickness of 2 * 6 mm were used, which were used for direct connection from the specified power source pv to the DC heater. A cycle separator was used to separate PV power from the refrigerator as needed or when converting from a DC system to an AC system to drive the refrigerator. To prepare for the four experiments, we connected 8 TPM-10 temperature sensors to each part of the system so that we could obtain accurate readings. At what locations were the temperature sensors placed in the freezer and refrigerator, the inlet and outlet of the condenser and absorber, the outlet of the mains, the inlet of the generator, and the eighth sensor that was used to monitor the temperature in the room in addition, a thermometer was used at the generator outlet so that the temperature could be monitored. In addition to using a meter to read the voltage, a meter was used to measure the DC, as shown in Figure 8. Figure 9 shows ceramic wool thermal in thermal insulator. Table 1 shows the Comparison between DC. ARS & AC.ARS for absorption refrigeration system.

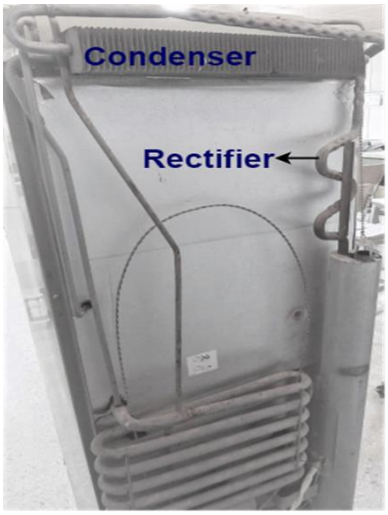

Fig. 4. A picture clip of the absorptive refrigeration system that was tested showing the rectifier and the condenser

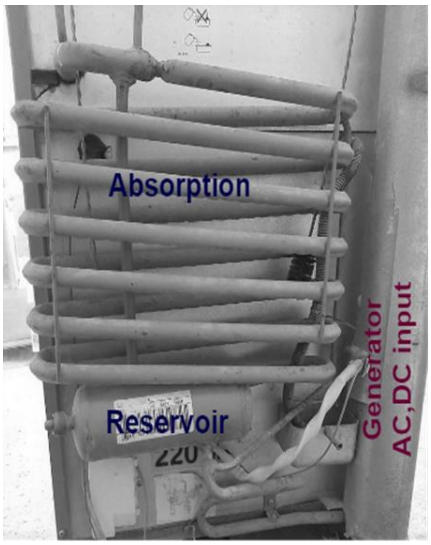

Fig. 5. A picture clip of the absorption refrigeration system that was tested, showing the absorber, the receiver, and the generator

Fig. 6. DC heater, 48 V, 450W

Fig. 7. Photovoltaic panel, nominal power 580W

Fig. 8. The thermal sensor panel connected to the refrigerator parts

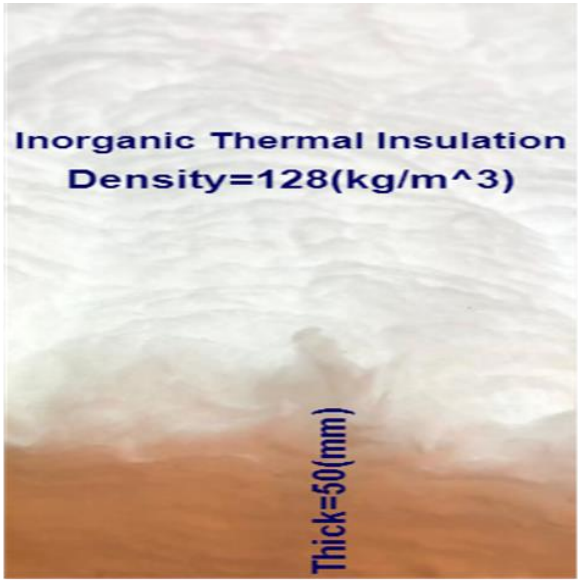

Fig. 9. Ceramic wool thermal in thermal insulator

Table 1
Comparison between DC. ARS & AC.ARS for absorption refrigeration system

Name	AC ARS	DC ARS	Unit
Voltage	220 –240	20-48	V
Current	1.4	8	A
Capacity	70	70	L
Condenser type	Finned type	Finned type	-
Dimension ($l * b * h$)	-	-	-
Insulation	-	-	-
Working Fluid	H2O-NH3	H2O-NH3	-

4. SAR System Thermodynamic Model

A straightforward thermodynamic model of the DAR cycle is used here to perform an analysis of the experimental findings. This model has been extensively cited in recent literature on DAR systems and has the potential to be applied to a diverse collection of DAR system configurations as a result of the straightforward character of the system's component submodels and the relative simplicity with which it can be put into practice., A. Najjaran, et al. [8] This section contains a description of the basic energy balance equations. In addition to the states that have been defined and their respective shown in Figure 1

$$\dot{Q}_{gen} - \dot{Q}_{loss} = \dot{m}_3 h_3 + \dot{m}_4 - \dot{m}_1 h_1 \quad (1)$$

The energy balance for the rectifier is given by Eq. (2). Q_{rect} is the heat rejected to the surroundings by the partial condensation of the vapor mixture's water portion. Between the incoming vapor mixture (State 4) and the departing condensate, vapor-liquid equilibrium is postulated (State 5). State 6 is near pure ammonia on its way to the condenser.

$$\dot{Q}_{rect} = \dot{m}_5 h_5 + \dot{m}_6 h_6 - \dot{m}_4 h_4. \quad (2)$$

The energy balance for the condenser is given by Eq. (3). The heat rejected to the surroundings by the condensation of the ammonia refrigerant (and any leftover water portion) at the system condensation pressure is denoted by Q ̇_"cond "

$$\dot{Q}_{cond} = \dot{m}_6(h_7 - h_6) \quad (3)$$

The liquid refrigerant flow rate entering the evaporator is considered the same as that exiting the condenser, $\dot{m}_6$ = $\dot{m}_7$ =$\dot{m}_9$. The energy balance for the evaporator in Eq. (4) takes into account both the precooling and evaporation processes, as well as the mass flows of refrigerant and inert gas (IG). The partial pressure and mass percentages of refrigerant and inert gas are

$$\dot{Q}_{evap} = \dot{m}_9(h_{10} - h_7) + \dot{m}_{ig}(h_{10,ig} - h_{8,ig}) \quad (4)$$

Calculated from the saturated vapor temperature at the evaporator output (State 10). In the absorber energy balance Eq. (5). The reservoir introduces refrigerant vapor mixed with inert gas from the bottom (State 10), while the reservoir introduces the weak solution from the top (State 8), the refrigerant absorbs into the weak solution, releasing heat into the surrounding environment (Cabs). and the remaining inert gas escapes at the absorber's top. It is assumed that the inert gas departs at the same temperature as the supplied weak solution, T_8 = T_8, ig,

$$\dot{Q}_{abs} = \dot{m}_{11}h_{11} - \dot{m}_{10}h_{10} - \dot{m}_8h_8 + \dot{m}_{ig}(h_{8,ig} - h_{10,ig}) \quad (5)$$

The energy balance for the liquid solution heat exchanger is given by Equation (6). Thermal energy is transmitted from the outer annulus's refrigerant-weak solution to the inner tube's refrigerant-rich solution. The model assumes no heat losses to the

$$\dot{m}_3h_3 + \dot{m}_5h_5 - \dot{m}_8h_8 = \dot{m}_1(h_1 - h_{11}) \quad (6)$$

The empirical functions of Patek and Klomfar are used to calculate the molar concentrations and specific enthalpies of the environment. ammonia-water combination under vapor-liquid equilibrium circumstances in Eq. (1)-(6). Finally, the coefficient of performance (COP) in Eq. (7) is the ratio of cooling output power at the evaporator to the heat input at the generator

$$COP = \frac{\dot{Q}_{evap}}{\dot{Q}_{gen}}. \quad (7)$$

4.1 Results and Discussion

Experimental measurements of four different experiments to operate an ARS solar absorption cooling system directly using a PV panel and a DC heater are plotted over the studied range of temperature input rates in the parts of the system.

4.1.1 The first experiment

In partly cloudy weather with little dust as shown in Figure 15. The output data was recorded every 4 minutes. For the parts of the system whose data are shown in the figures and curves below, for each part independently as shown in Figure 9, 10, 11, 12, 13, 14, and 15, from this (first), the

temperature of the cooled space was maintained at 32 °C ± 1 °C. for 4 hours. It is possible to compare the decrease in the temperature in the evaporator of the system with the increase in the temperature entered in the generator as shown in Figure 16 through a DC heater that operates with a capacity of 450 watts. The new and distinctive thing in this experiment is that the fluctuation of the DC voltage as a result of clouds and dust does not affect It significantly affects the work of the heater, which supplies the generator with thermal energy, and thus does not affect the work of the refrigerator much. The ARS solar system can be operated in different weather conditions, as shown in a three-dimensional way in Figure 17. It is noted that the temperature decreases and increases as a result of the fluctuation of the voltage difference as a result of clouds and dust at higher values of temperature in the generator, and this corresponds to the operating conditions in which the generator is delivered The maximum flow rate of ammonia gas vapor from the rectifier to the condenser, at values above Q_{gen}. Which a DC system's evaporator and generator temperatures do not limit the specific cooling outputs that can be achieved. at low values of Q_{gen}. Figure 16 depicts a temporal comparison of the evaporator and generator temperatures in a DC system. During the operation of the system, the generator temperature gradually rises. The evaporator temperature drops as the generator temperature rises. When the generator temperature reached 50 °C, the evaporator temperature began to drop. The fridge took less than 20 minutes to start cooling. When the generator temperature reaches the optimum level, the lowest evaporator temperature of 16.4 °C was obtained in this experiment during approximately 4 hours in partly cloudy and dusty weather. Through this experiment, it was concluded that if the experiment takes a longer time, the temperature in the evaporator decreases. The generator temperature rises, which we proved in the subsequent experiments. The first experiment took place on September 21, for a period between 9:15 am and 1:15 pm. Figure 18 shows a comparison between the generator temperature and evaporator temperature during 232 minutes.

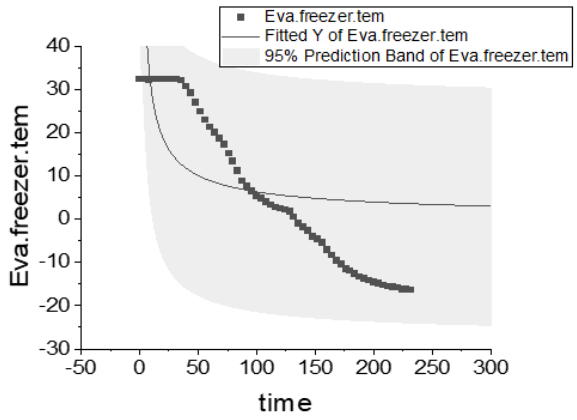

Fig. 10. Evaporator temperature data

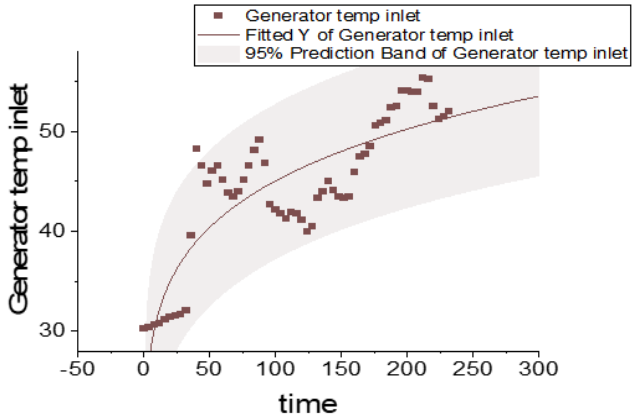

Fig. 11. Temperatures at the inlet of the generator

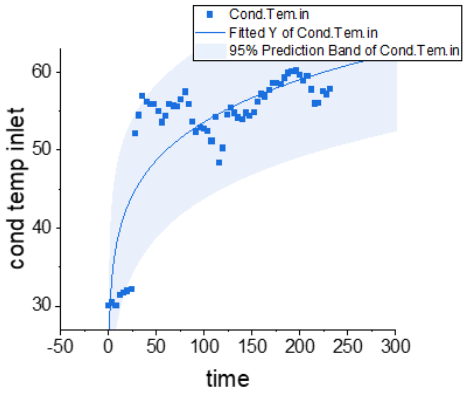

Fig. 12. Condenser inlet temperature

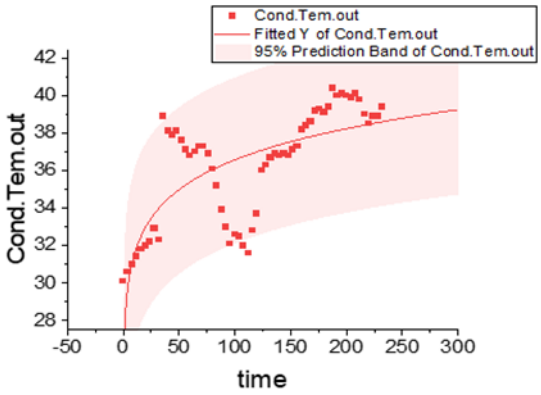

Fig. 13. Temperatures at the outlet of the condenser

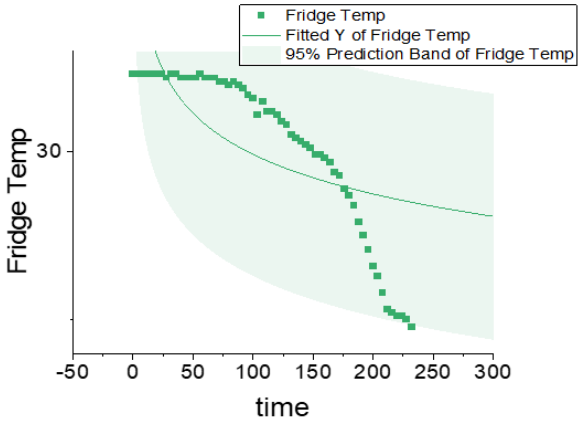

Fig. 14. Temperatures at the Fridge

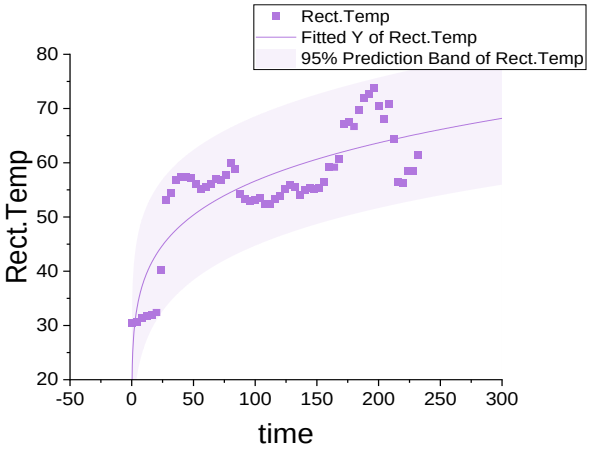

Fig. 15. Temperatures at the rectifier

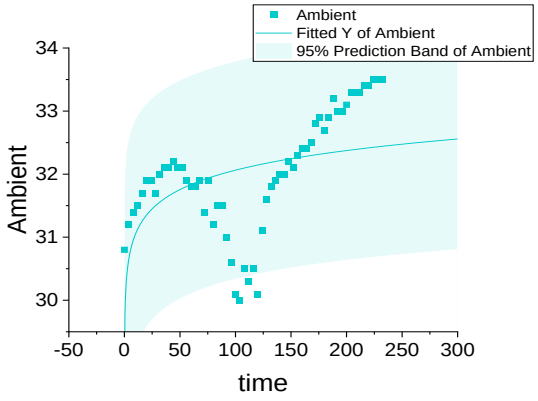

Fig. 16. Ambient temperature of the system

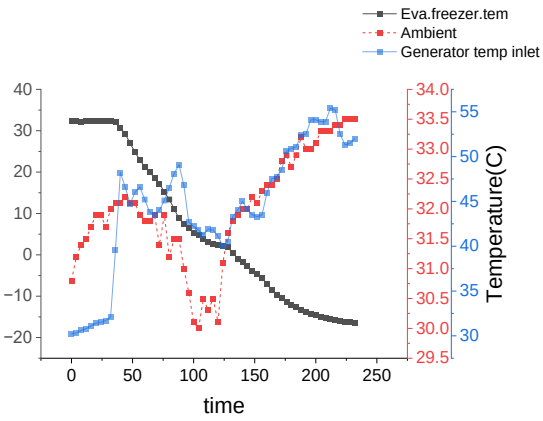

Fig. 17. Comparison of generator temperature and room temperature around the refrigerator

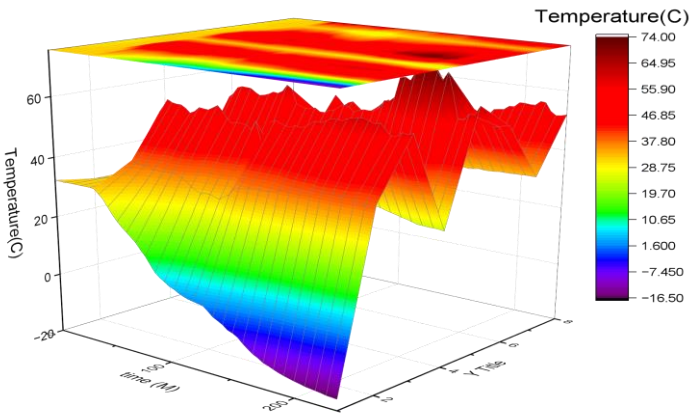

Fig. 18. 3D models. A comparison between the generator temperature and evaporator temperature during 232 minutes

4.1.2 The second experiment

In the second experiment of the same month, the room temperature was set to 25.6 ° C in clear weather, and after 156 minutes of operation, that is, after about two and a half hours from 10 am to 12:30 pm. The temperature in the evaporator reached -19.4 ° C, using 580 W photovoltaic panels and a 450-watt heater to power the ARS solar system. The voltage and current data are also shown in Figure 19, which shows the operation of the refrigerator normally through a gradual decrease in voltage and current as a result of the high temperatures in the generator and from Figure 20 and Figure 21, we observe that the higher the temperatures in the generator, the lower the temperatures in the evaporator and refrigerator. Feeds the current heater Continuous generator with the necessary thermal energy. From Figure 22 and Figure 23, it is possible to observe the temperature input of the generator compared to the temperatures in the evaporator and other devices and its effect on the COP performance coefficient, we note that the higher the temperatures in the generator, the lower the temperatures in the evaporator and the impact on the performance coefficient and efficiency of the refrigerator. So, it was clear that the ambient temperatures of the cooling system using solar energy and the weather quality compared to the first experiment, the results do not vary much, this proves once again that voltage fluctuations due to Clouds or dust are no different. Significantly affect the performance of solar ARS. Output data is recorded every 4 minutes. This experiment was conducted on September 26, 2022. In addition to the practical experiments, the second experiment was simulated using the EES program through the temperature data of refrigerator parts obtained from the practical experiment in the laboratory, as well as the average concentration of ammonia. In water estimated at 30% according to the specifications of the refrigerator manufacturer The temperature, pressure, and saturation temperature of all parts of the refrigerator were calculated. Figure 24 shows the output temperature of the generator and the temperature of the evaporator as well as the room temperature compared to the capacity of the generator. Figure 25 shows the effect of Q_ gen on the performance modulus (COP). The mass flow rate of the refrigerator parts was calculated, as shown in Figure 26. Also, the generator input temperatures and low temperatures in the evaporator were compared in three dimensions, as shown in Figure 27. During 156 minutes, we observed the flow from the refrigerator in clear weather. It is possible to see the temperatures of the entire system parts in Figure 28. All the above calculations and comparisons were made based on the temperatures of each part. Independently. Grades Heat

various appliances such as freezer, refrigerator, condenser, absorption vessels, generator, and rectifier. And also, the voltage and current data as shown in Figure 29 to 39,

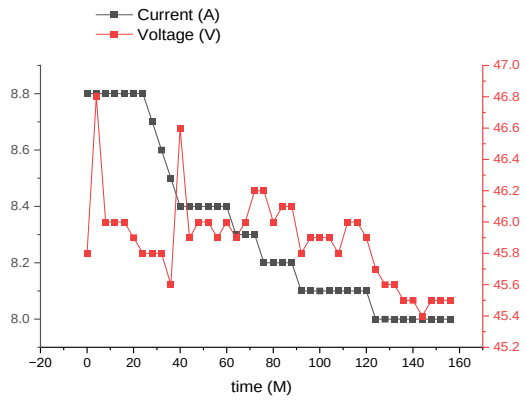

Fig. 19. Comparison between the voltage and current of the DC heater during the operation of the ARS system

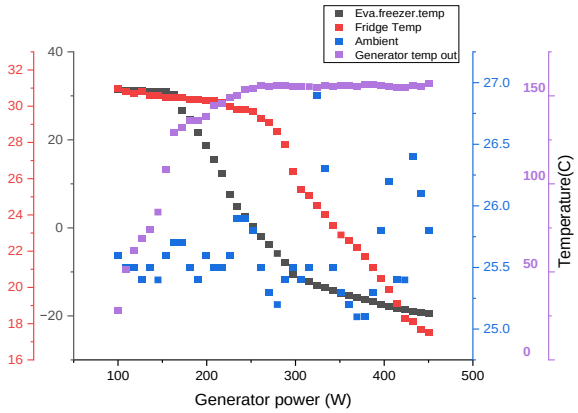

Fig. 20. Comparison of the temperatures of the generator, evaporator, condenser temperature, and rectifier, as well as room temperature through 15

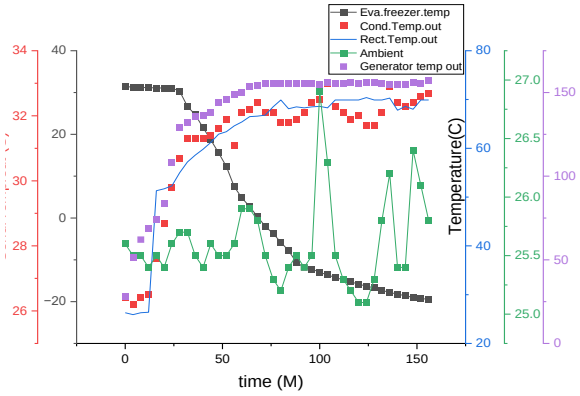

Fig. 21. Comparison of the temperatures of the generator, evaporator, condenser temperature, and rectifier, as well as room temperature through 15

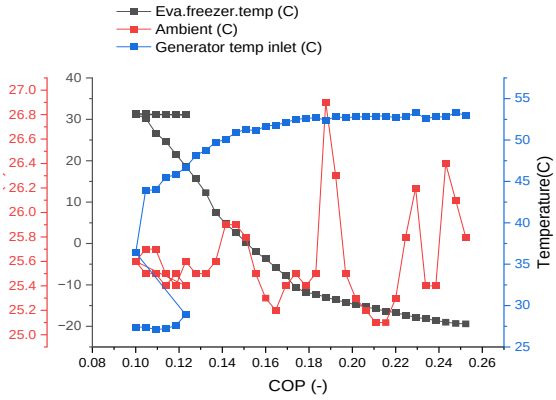

Fig. 22. simulation using the EES program for the value of COP through temperature and its effect on room temperature

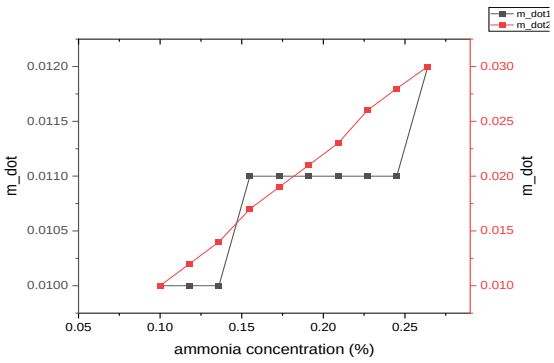

Fig. 23. A comparison of the COP value, the generator entry temperature, and the condenser entry temperature, in addition to the temperatures in the absorption vessel, the room temperature

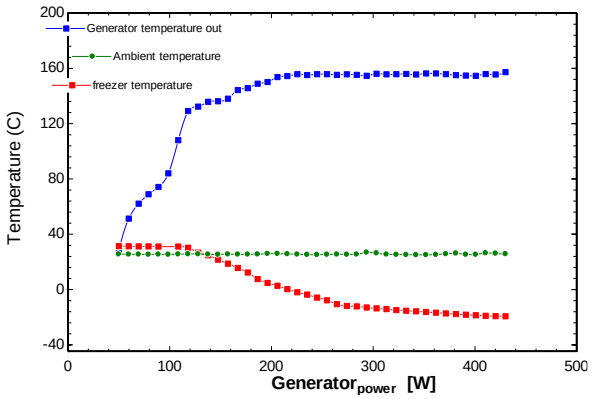

Fig. 24. A comparison of the COP value, the generator entry temperature, and the condenser entry temperature, in addition to the temperatures in the absorption vessel, and the room temperature

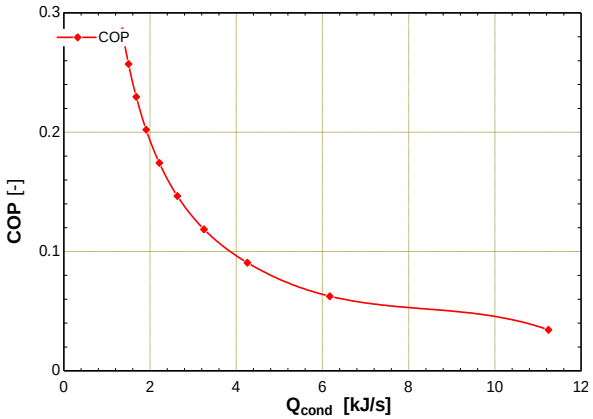

Fig. 25. The effect of Q_gen on the coefficient of performance (COP)

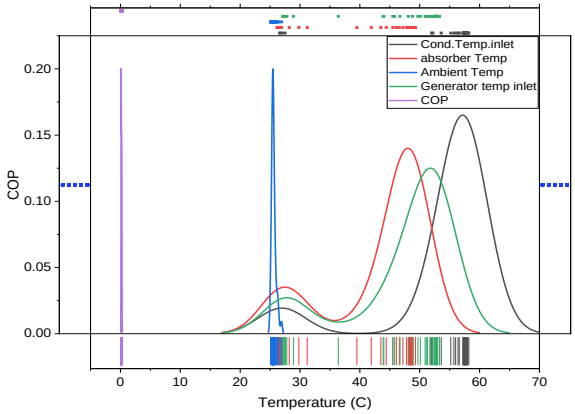

Fig. 26. The mass flow rate of the system compared to the average concentration of ammonia in the water

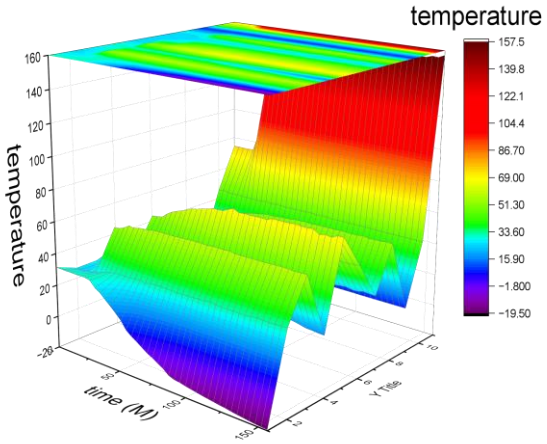

Fig. 27. 3 D model of input temperature in the generator and temperatures in the evaporator of the S.ARS solar absorption refrigerator during 156 minutes

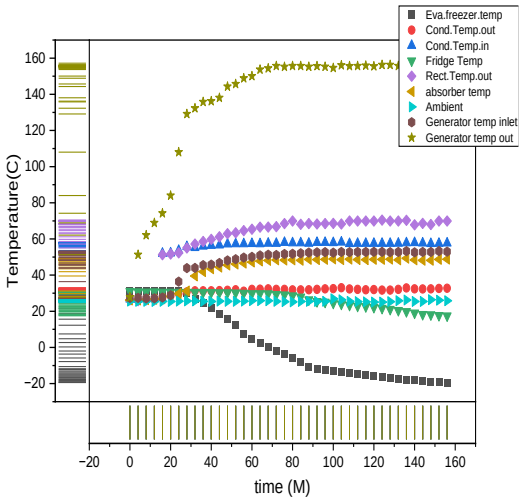

Fig. 28. These curves represent the temperature data in all parts of the solar refrigerator

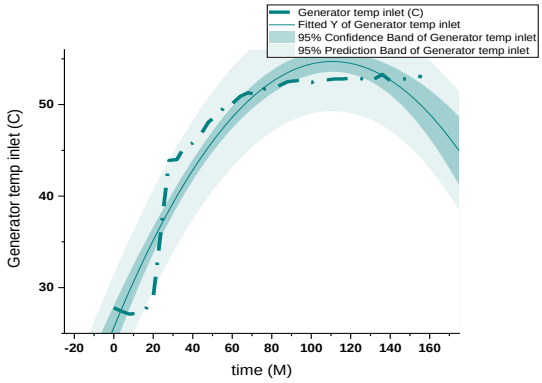

Fig. 29. Generator temperature entry data during 156 minutes of the second experiment

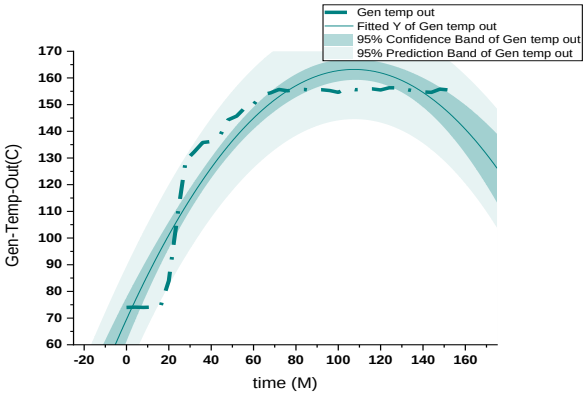

Fig. 30. Curve of generator output temperature data

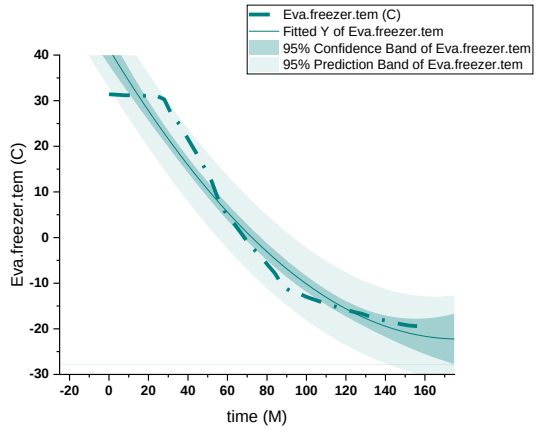

Fig. 31. Evaporator temperature data during 156 minutes of the second experiment

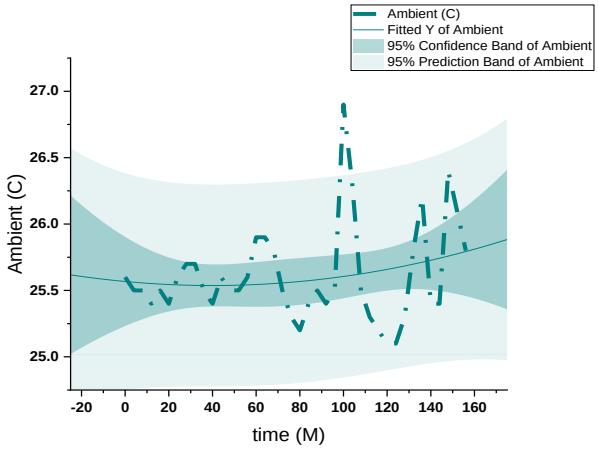

Fig. 32. Room temperature data during the second experiment

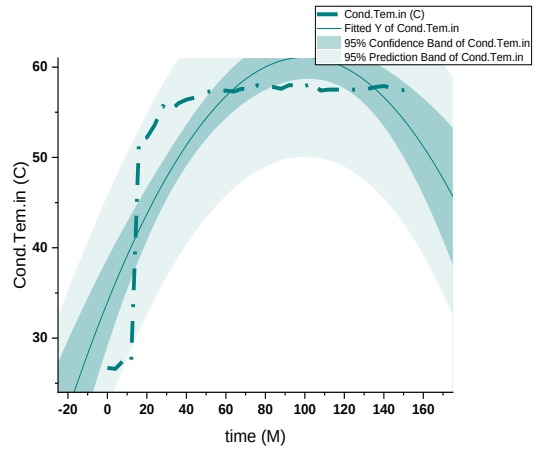

Fig. 33. Inlet condenser temperature data during 156 minutes of the second experiment

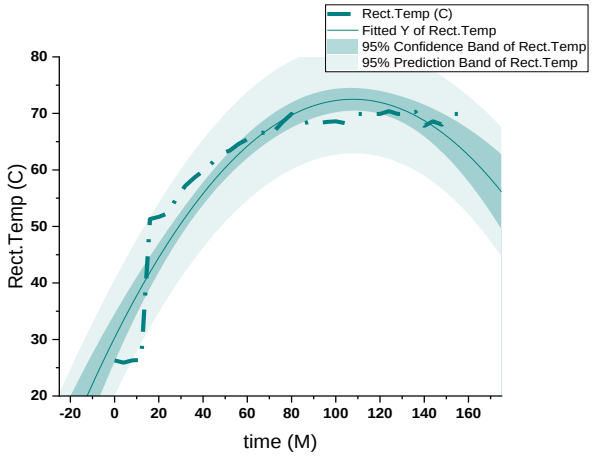

Fig. 34. Rectifier temperature data during 156 minutes of the second experiment

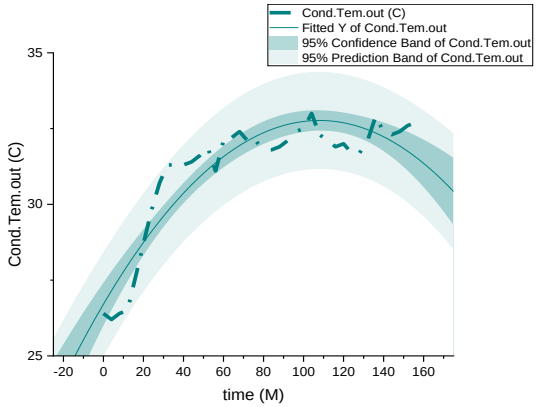

Fig. 35. Condenser temperature output data after 156 minutes during the second experiment

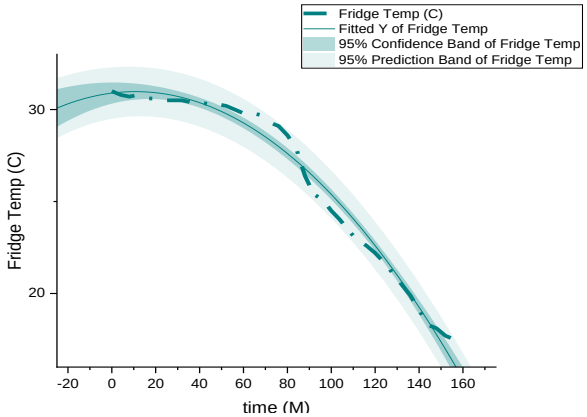

Fig. 36. Fridge temperature data during 156 minutes of the second experiment

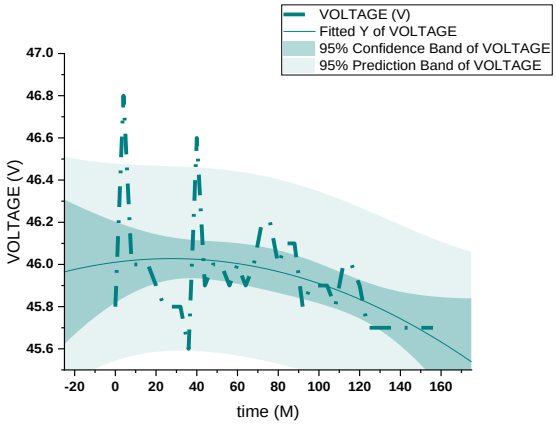

Fig. 37. data of the voltage consumed by the electric heater in the during 156

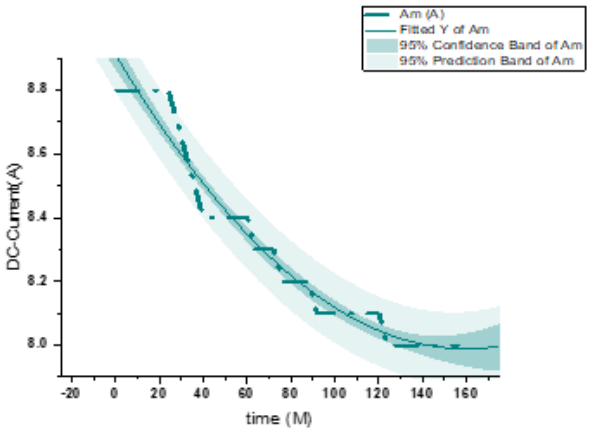

Fig. 38. DC data consumed by the refrigerator during 156 minutes

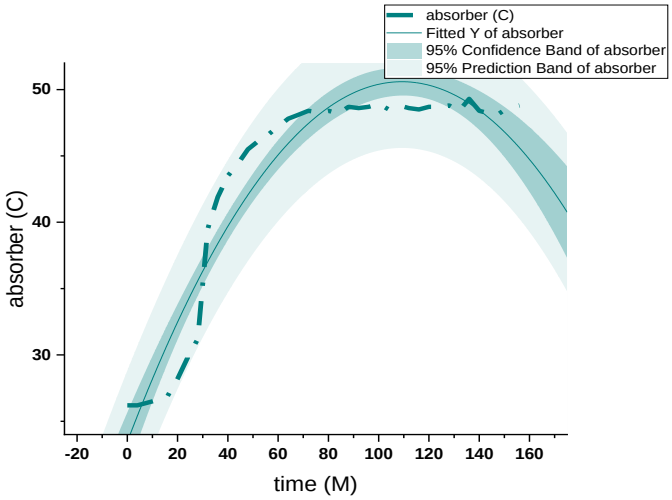

Fig. 39. Absorber temperature curve after 156 minutes in the second experiment

4.1.3 Third experiment

In this experiment, the solar ARS was powered on November 19 from 8:30 am to November 20 at 8:30 am with an electric source (AC) as Figure 40 shows, then the drive system was switched to (DC) from 8 30 a.m. from November 20 to 22 at 8:30 a.m. for the year 2022, as shown in Figure 41

and Figure 42. We also see in Figure 43 a three-dimensional model of the third experiment for a period of 3 days. On the first day of this experiment, after 178 minutes of work, we reached -19 inside the evaporator compared to the previous (second) experiment. This result was reached within 152 using photovoltaic energy directly. Moreover, on the first day of this experiment also, a temperature of -27 °C was observed in the evaporator. And after converting the operating system to a solar photovoltaic source directly (DC), it was also observed that the refrigerator continues to work with the same efficiency, and -27 ° C was observed in the evaporator for more than 7 consecutive hours of our experiment on the second day. There is not much difference in the way both systems operate, and this allows the AC system to be interchangeable with the solar PV direct current (DC) system to drive the ARS absorption refrigeration system. Which leads to a significant reduction in the costs of energy production, storage and maintenance, and also helps to reduce emissions, environmental pollution and global warming, unlike compression cooling systems. The temperatures obtained in both AC and DC systems are sufficient for storing different types of food, in addition to storing vaccines and medicines that need to be stored at lower temperatures. Solar absorption cooling technology can be delivered to rural and remote areas where it is difficult to supply electric power grids. The use of DC electricity for heating is not restricted if the voltage fluctuates slightly due to draft or dust, unlike a compressor which needs a steady, stable electrical supply. In compressive systems. Figure 44 shows the temperature data are shown in the curves for three consecutive days of the third experiment, that is, during the 72 hours of continuously.

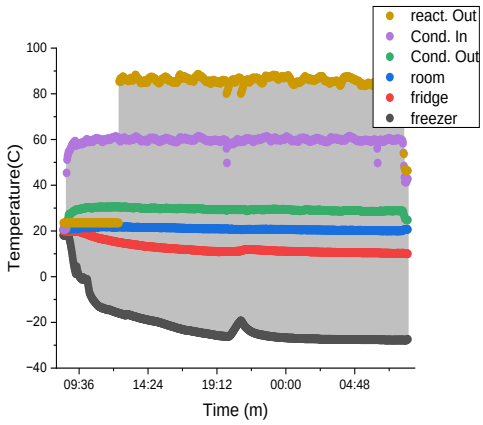

Fig. 40. Temperature data are shown in the curves on the first day of the third experiment, that is, during the first 24 hours

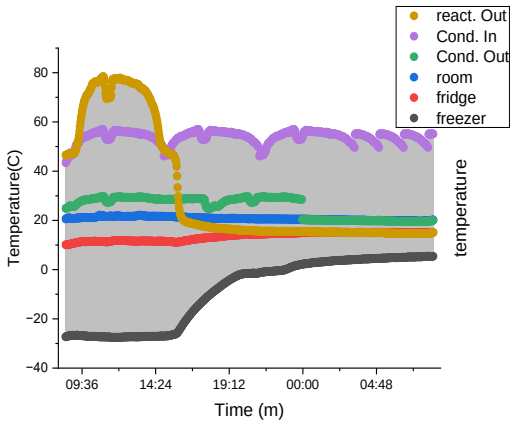

Fig. 41. Temperature data are shown in the curves on the second day of the third experiment, during the second 24 hours

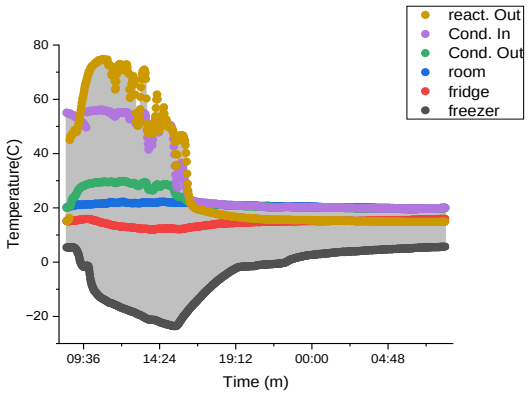

Fig. 42. Temperature data for the parts of the system from the third day of the third experiment, during the 24 hours

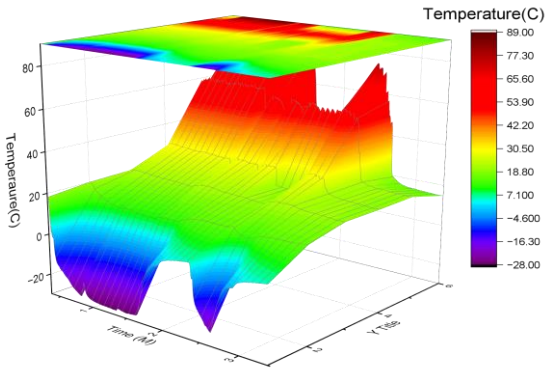

Fig. 43. A three-dimensional model for the third experiment during 3 day

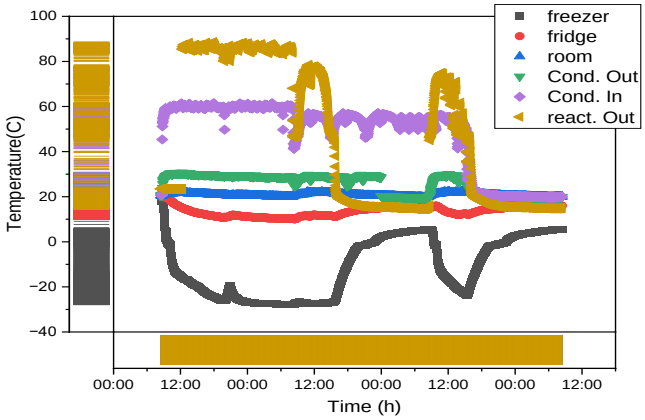

Fig. 44. The temperature data are shown in the curves for three consecutive days of the third experiment, that is, during the 72 hours of continuously

4.1.4 Fourth experiment

This experiment was conducted on December 17, 2022, from 8:38 am to the next day 10 pm continuously. The photovoltaic panel is set at an the angle of (30) degrees in terms of the intensity of solar radiation, using the temperature data shown in the curves for the experiment for a period of 2246 minutes, equivalent to 37 hours, as in Figure 44. After (7) hours had passed, the temperature began to drop below zero degrees Celsius until it reached (-16) in the evaporator for the first day, as shown in Figure 45. A degree below zero Celsius is maintained until 6:30 in the evening, then the temperatures begin to rise gradually to a maximum of 8 degrees Celsius the next day at 8:30 in the morning, and then begin to decrease again as shown in Figure 46. Through these temperatures, food, food, medicines, vaccines, etc. can be preserved. Sub-zero temperatures can be kept by producing ice during the day and using it for cooling at night, or by using batteries to store energy during the day and use it at night. The temperatures of most parts of the refrigerator are measured using dual temperature sensors. Parameterization was taken every 2 minutes using an automated data logger. The experiment was repeated two days later, on December 20, 2022, but the angle was changed to an angle of 20 degrees, and the parameter was taken to take temperature measurements every (2) minutes for most parts of the system. We noticed that after the passage of (7) in the evaporator (-24) for the first day, as shown in Figure 47, we can conclude that adjusting the PV at an angle (20) is

better than adjusting it at an angle (30), so through these experiments it is possible to reduce the percentage of consumption Electric energy (AC) by (50) % during daylight hours, relying on photovoltaic energy to directly operate cooling and refrigeration systems, and through the four experiments, it was shown that. Photovoltaic energy can be used through photovoltaic systems to operate absorption ice systems directly and eliminate the costs of parts used in converting power from direct current to alternating current, and maintenance costs also for 24 hours, which reduces harmful environmental effects and reduces global warming, and reduces. The costs of producing electrical energy are to a large extent consumed in the operation of refrigeration systems and compressive refrigeration systems. Figure 48 shows temperature data for system components in curves over 2700 minutes. within 45 hours.

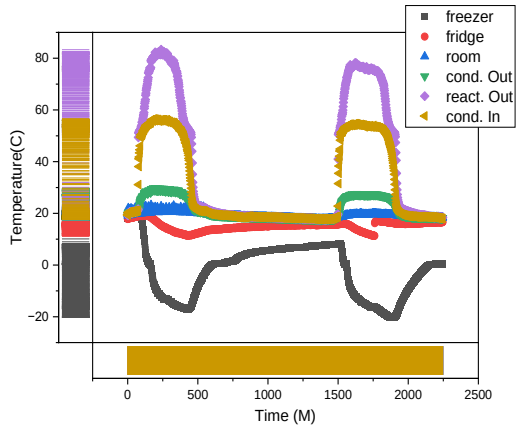

Fig. 45. Temperature data for system components for 2246 minutes

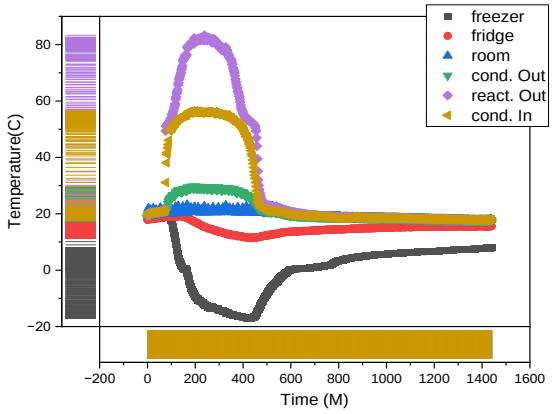

Fig. 46. Comparison of the temperatures of the components of the system during 1440 minutes

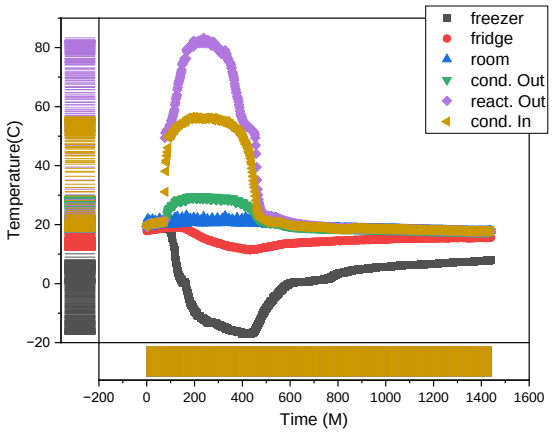

Fig. 47. Temperature data within 800 minutes for the second day within the last 13 hours

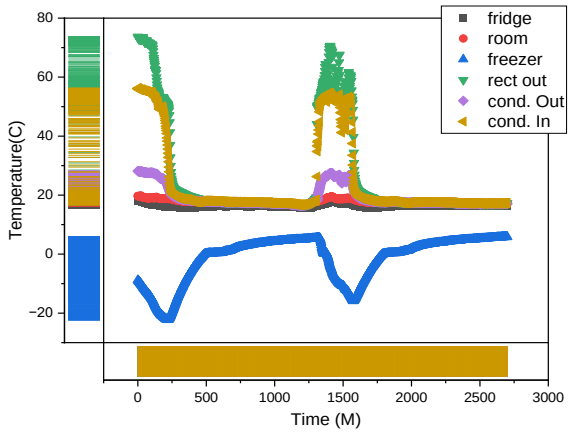

Fig. 48. Temperature data for system components in curves over 2700 minutes within 45 hours

5. Conclusion

The findings of this study are very interesting. Moreover, the investing of using renewable energy resources is very significant, especially with these fossil fuel resources crises. Furthermore, the consequences of using fossil fuel are global warming and environment pollution. Therefore, this outcome of this study could be summary as following

i. The possibility of significantly reducing material costs by dispensing with the use of transformers and storing energy through
ii. the use of an electric heater that operates with a direct current system with the specifications that were designed to heat the generator by harnessing the output of photovoltaic energy directly to the drive the system, knowing that this system does not It contains no compressor, so no gases that pollute the environment and cause global warming are used.
iii. To drive the system, compressive cooling systems that operate with alternating current are adhered to with a constant voltage; also, through experiments, it was discovered that adjusting the PV panel at an angle of 20 degrees gives the best results in the work of the system. During multiple tests, the refrigerator's evaporator temperature reached -26°C and the compartment temperature was around 10°C.
iv. The performance of this refrigerator using the PV panel was similar to the performance of it with a conventional electric source (AC).

Acknowledgement
This research was not funded by any grant.

References

[1] Esfanjani, Pouya, Sajjad Jahangiri, Ali Heidarian, Mohammad Sadegh Valipour, and Saman Rashidi. "A review on solar-powered cooling systems coupled with parabolic dish collector and linear Fresnel reflector." *Environmental Science and Pollution Research* 29, no. 28 (2022): 42616-42646. https://doi.org/10.1007/s11356-022-19993-3
[2] Narváez-Romo, Beethoven, Eliane Hayashi Suzuki, and José R. Simões-Moreira. "A comparative study of solar cooling technologies." In *CLIMA 2022 conference*. 2022.
[3] Mehrpooya, Mehdi, Bahram Ghorbani, and Seyed Sina Hosseini. "Thermodynamic and economic evaluation of a novel concentrated solar power system integrated with absorption refrigeration and desalination cycles." *Energy Conversion and Management* 175 (2018): 337-356. https://doi.org/10.1016/j.enconman.2018.08.109
[4] Ozgoren, Muammer, Mehmet Bilgili, and Osman Babayigit. "Hourly performance prediction of ammonia–water solar absorption refrigeration." *Applied Thermal Engineering* 40 (2012): 80-90. https://doi.org/10.1016/j.applthermaleng.2012.01.058
[5] Selvaraj, Divya Arputham, and Kirubakaran Victor. "Design and performance of solar PV integrated domestic vapor absorption refrigeration system." *International Journal of Photoenergy* 2021 (2021): 1-10. https://doi.org/10.1155/2021/6655113
[6] Dhindsa, Gurprinder Singh. "Review on performance enhancement of solar absorption refrigeration system using various designs and phase change materials." *Materials today: proceedings* 37 (2021): 3332-3337. https://doi.org/10.1016/j.matpr.2020.09.125
[7] Najjaran, Ahmad, James Freeman, Alba Ramos, and Christos N. Markides. "Experimental investigation of an ammonia-water-hydrogen diffusion absorption refrigerator." *Applied energy* 256 (2019): 113899. https://doi.org/10.1016/j.apenergy.2019.113899
[8] Bellos, Evangelos, Ion Chatzovoulos, and Christos Tzivanidis. "Yearly investigation of a solar-driven absorption refrigeration system with ammonia-water absorption pair." *Thermal Science and Engineering Progress* 23 (2021): 100885. https://doi.org/10.1016/j.tsep.2021.100885
[9] Khan, Mohammed Mumtaz A., R. Saidur, and Fahad A. Al-Sulaiman. "A review for phase change materials (PCMs) in solar absorption refrigeration systems." *Renewable and sustainable energy reviews* 76 (2017): 105-137. https://doi.org/10.1016/j.rser.2017.03.070
[10] Khan, Muhammad Saad, Sambhaji T. Kadam, Alexios-Spyridon Kyriakides, Athanasios I. Papadopoulos, Ibrahim Hassan, Mohammad Azizur Rahman, and Panos Seferlis. "A new correlation for performance prediction of small and large capacity single-effect vapor absorption refrigeration systems." *Cleaner Energy Systems* 1 (2022): 100002. https://doi.org/10.1016/j.cles.2022.100002
[11] Sözen, Adnan, Tayfun Menlik, and Engin Özbaş. "The effect of ejector on the performance of diffusion absorption refrigeration systems: An experimental study." *Applied thermal engineering* 33 (2012): 44-53. https://doi.org/10.1016/j.applthermaleng.2011.09.009

[12] Martínez-Maradiaga, David, Joan Carles Bruno, and Alberto Coronas. "Steady-state data reconciliation for absorption refrigeration systems." *Applied Thermal Engineering* 51, no. 1-2 (2013): 1170-1180. https://doi.org/10.1016/j.applthermaleng.2012.10.027
[13] Bhat, Sunil, and H. Adarsha. "A short review on utility of solar energy in refrigeration and fabrication of a mini solar fridge."
[14] Najjaran, Ahmad, Asmaa A. Harraz, N. Mac Dowell, and C. N. Markides. "Numerical and experimental investigation of diffusion absorption refrigeration systems for use with low-temperature heat sources." *Proc ECOS* (2018): 17-22.
[15] Yousuf, Noman, Etienne Biteau, Timothy Anderson, Michael Gschwendtner, and Roy Nates. "Modelling the performance of a diffusion absorption refrigeration system." (2014).
[16] Jemaa, Radhouane Ben, Rami Mansouri, Ismail Boukholda, and Ahmed Bellagi. "Experimental characterization and performance study of an ammonia–water–hydrogen refrigerator." *international journal of hydrogen energy* 42, no. 13 (2017): 8594-8601. https://doi.org/10.1016/j.ijhydene.2016.06.150
[17] Taieb, Ahmed, Khalifa Mejbri, and Ahmed Bellagi. "Detailed thermodynamic analysis of a diffusion-absorption refrigeration cycle." *Energy* 115 (2016): 418-434. https://doi.org/10.1016/j.energy.2016.09.002
[18] de Rezende, Túlio Tito Godinho, Flavio Neves Teixeira, Jose Antonio da Silva, Luiz Gustavo Monteiro Guimarães, and Matheus dos Santos Guzella. "A non-intrusive method for evaluation ammonia mass flow rate in the condenser for diffusion-absorption refrigerators." *Flow Measurement and Instrumentation* 72 (2020): 101695. https://doi.org/10.1016/j.flowmeasinst.2020.101695
[19] Farzadi, Ramin, and Majid Bazargan. "Experimental study of a diffusion absorption refrigeration cycle supplied by the exhaust waste heat of a sedan car at low engine speeds." *Heat and Mass Transfer* 56, no. 4 (2020): 1353-1363. https://doi.org/10.1007/s00231-019-02793-w
[20] Al-Samari, Ahmed, Yasseen AJ Almahdawi, and Laith Abd hasnawi Al-Rubaye. "Design of absorption refrigeration system using solar energy resource." *International Journal of Air-Conditioning and Refrigeration* 28, no. 03 (2020): 2050025. https://doi.org/10.1142/S201013252050025X
[21] Salman, Tabarek Daood, and Ahmed Al-Samari. "Experimental Performance Evaluation of Absorption Refrigeration System Driven by Waste Heat of Engine Exhaust." *Diyala Journal of Engineering Sciences* (2022): 75-84. https://doi.org/10.24237/djes.2022.15308
[22] Armaroli, Nicola, and Vincenzo Balzani. "Solar electricity and solar fuels: status and perspectives in the context of the energy transition." *Chemistry–A European Journal* 22, no. 1 (2016): 32-57. https://doi.org/10.1002/chem.201503580
[23] Razali, Nizamuddin, Mohd Bekri Rahim, and Sri Sumarwati. "Influence of Volume Fraction of Titanium Dioxide Nanoparticles on the Thermal Performance of Wire and Tube of Domestic Refrigerator Condenser Operated with Nanofluid." *Journal of Advanced Research in Numerical Heat Transfer* 11, no. 1 (2022): 12-22.
[24] Ilham, Zul. "Multi-criteria decision analysis for evaluation of potential renewable energy resources in Malaysia." *Progress in Energy and Environment* 21 (2022): 8-18. https://doi.org/10.37934/progee.21.1.818
[25] Talal, Wadah, and Abdulrazzak Akroot. "Exergoeconomic Analysis of an Integrated Solar Combined Cycle in the Al-Qayara Power Plant in Iraq." *Processes* 11, no. 3 (2023): 656. https://doi.org/10.3390/pr11030656
[26] Ahmad, Saif Nawaz, and Om Prakash. "Optimization of Earth Air Tube Heat Exchanger for Cooling Application Using Taguchi." *Journal homepage: http://iieta. org/journals/ijht* 38, no. 4 (2020): 854-862. https://doi.org/10.18280/ijht.380411